IEEE Systems Journal, Volume 14, Issue 2, June 2020, pp. 2694-2702
DOI:10.1109/JSYST.2019.2932897

Robust Optimisation based Energy Storage Operation for System Congestion Management

Xiaohe Yan, *Student Member*, Chenghong Gu, *Member, IEEE*, Xin Zhang, *IEEE*, Furong Li, *Senior Member, IEEE*

***Abstract*—Power system operation faces an increasing level of uncertainties from renewable generation and demand, which may cause large-scale congestion under ineffective operation.**

This paper applies energy storage (ES) to reduce system peak and congestion by robust optimisation, considering the uncertainties from ES State of Charge (SoC), flexible load, and renewable energy. First, a deterministic operation model for ES, as a benchmark, is designed to reduce the variance of branch power flow based on the least-square concept. Then, a robust model is built to optimise ES operation with the uncertainties in the severest case from load, renewable and ES SoC that are converted into branch flow budgeted uncertainty sets by the cumulant and Gram-Charlier expansion method. The ES SoC uncertainty is modelled as an interval uncertainty set in the robust model, solved by duality theory. These models are demonstrated on a grid supply point (GSP) to illustrate the effectiveness of congestion management technique. Results illustrate that the proposed ES operation significantly improves system performance in reducing system congestion. This robust optimisation based ES operation can further increase system flexibility to facilitate more renewable energy and flexible demand without triggering large-scale network investment.

***Index Terms*— System congestion, load uncertainty, energy storage, robust optimisation**

I. Introduction

DUE to the ageing infrastructure and limited capacity of existing energy systems, a huge amount of renewable energy is wasted worldwide. In 2015, the cost of wind curtailment exceeded £90 million from 1.3GWh energy waste in the UK [2]. Energy storage (ES) is able to address system congestion by temporally shifting power to relieve the pressure on system constraints, facilitating renewable energy penetration. Paper [3] uses ES to shave demand peak and regulate frequency, but not accurately addresses system overloading issues. Paper [4] uses economic signals to guide ES operation, but this approach is less efficient when the price peaks do not match power peaks.

There are many commercial and technical barriers that obstacle the utilisation of ES in the power system, including 1) the pricing signals for ES should be clear and incentive. Currently, ES does not receive sufficient incentives, where the main profit is from energy arbitrage. For example, the benefits from reducing system congestion and peak power flow could be rewarded to ES if they provide the services; 2) the uncertainties in power systems should be considered in ES operation. With uncertain generation and demand, it is more complexed to design ES operating strategies. The inaccuracy in ES operation would even exacerbate system congestions and energy balancing. ESs are normally operated by deterministic optimal models [5-7], without considering uncertainties from flexible load and renewable generation. Although some research work considers renewable power uncertainties [8], the impact of ES operation on network congestion is not properly considered.

The uncertainties of active load and renewable energy generation lead to unexpected system peak and uncontrollable network congestions, which increases system risks and associated operation cost. It would bring forward network reinforcement time and increases operation cost in the long run. Thus, it is important to consider uncertainties in utilising ES to reduce system congestion. The uncertainties are mainly from three sources: ES, and flexible load and renewable generation. To model power flows considering uncertainties flexible load and renewable generation, there are two key methods: Monte-Carlo simulation and probability theory. Papers [9-11] use Monte-Carlo simulation to determine the probabilistic power flows, but they are not applicable to large-scale systems. The probability methods are based on a various combination of expansion approximations, cumulant and moment to determine the optimal probabilistic power flow in [12-14].

In terms of optimisation with uncertainties, generally, there are two approaches, which are the stochastic programming [15] and robust optimisation [16, 17]. Robust optimisation methods consider uncertain parameters by taking values within known confidence bounds, which are generally easy to obtain. Because network reinforcement is determined by peak branch power flow, robust optimisation can minimise system peak under high uncertainties to reduce system congestion, deferring network reinforcement horizon. There are several papers applying robust optimisation to system operation considering uncertainties from the load, renewable output and energy prices. Paper [18, 19] propose a second-order cone programming robust optimisation under uncertainties to reduce the uncertainty and uses a two-stage robust centralised-optimal dispatch model under uncertain PV output. For the uncertainty sets in robust optimisation, box and budgeted uncertainty sets are widely used. Papers [20, 21] consider budgeted uncertainty sets in modelling. The correlation between load and wind

uncertainties are considered by budget constraints [20]. Paper [21] converts the max-min problem to a Mixed Integer Programming (MIP) problem using Binary Expansion, accommodating uncertain renewable in the Security-Constraint Unit Commitment (SCUC). With robust models, the problem is solved by Benders Decomposition [20] and column-and-constraint generation algorithm [18, 22, 23]. However, these methods are not for operating ES, whose uncertainty in State of Charge (SoC) significantly impact operation.

This paper designs a novel operation method for ES dispatch by the system operator to reduce the variances of branch flows. The branches with high asset cost have the priority to use the ES to reduce their power flow variances because their high power flow levels lead to nearer reinforcement horizon and high investment cost. By considering the uncertainties of flexible load, renewable energy, and ES SoC, robust optimisation is applied to operate ES to shift the peak power flow to valley periods. Load and generation uncertainties are converted into branch flow uncertainties as budgeted sets by applying the cumulant and Gram-Charlier expansion method. The ES SoC uncertainty is modelled as an interval set in the robust optimisation. The constraints of power flow, SoC, and Charing/Discharging (C/D) rate are applied in robust optimisation. The proposed method is demonstrated on a practical Grid Supply Point (GSP) from UK distribution system.

The main contributions of this paper are: i) it proposes a new C/D model based on least-square to reduce branch flow variances from uncertainties of flexible load and renewable energy; ii) it designs a robust optimisation model to operate ES by considering all uncertainties of flexible load, renewable energy, and ES SoC; and iii) it compares the performance of deterministic and robust models under different uncertainty levels in terms of system peak and congestion reduction.

The rest of the paper is organised as follows: Section II describes the process to determine probabilistic power flow based on demand and renewable generation uncertainty. Section III proposes a deterministic model and robust optimisation models for ES operation. Section IV demonstrates and compares the proposed deterministic and robust models on a local GSP distribution network. Section V draws conclusions.

II. Probabilistic Power Flow with Demand and Generation Uncertainty

Probabilistic power flow is proposed to capture the uncertainties from flexible load and renewable for robust optimisation. Based on the DistFlow model, the uncertainties are transferred to power flow by using the combined cumulant and Gram-Charlier expansion method.

A. Power Flow Linearisation

In the cumulant method for probabilistic power flow analysis, the linear combination of independent variables is considered. In the distribution network, especially radial ones, the DistFlow model [24, 25] is widely used to simplify the relationship between branch power flow and nodal power change, which is modelled as:

$$P_{l+1} = P_l - \frac{r_l \times (P_l{}^2 + Q_l{}^2)}{V_l{}^2} - p_{i,l} \quad (1)$$

$$Q_{l+1} = Q_l - \frac{x_l \times (P_l{}^2 + Q_l{}^2)}{V_l{}^2} - q_{i,l} \quad (2)$$

$$V_{l+1}{}^2 = V_l{}^2 - 2(r_l \times P_l + x_l \times Q_l) + \frac{(P_l{}^2 + Q_l{}^2)(r_l{}^2 + x_l{}^2)}{V_l{}^2} \quad (3)$$

where P_l and Q_l are active and reactive power flows in branch l; the branch impedance is presented as $z_l = r_l + jx_l$.

To comply with the system operating standard, the nodal voltage in the distribution network should be within a certain range, set as $V_l \subset [0.95, 1.05]$. Because the nonlinear parts of the nodal voltage are much smaller than the linear parts, and thus $(P_l{}^2 + Q_l{}^2)(r_l{}^2 + x_l{}^2)/V_l{}^2$ can be ignored [25, 26]. By assuming nodal voltage at the nominal level is $1\,\text{p.u.}$, $(V_l - 1)^2 = V_l{}^2 - 2V_l + 1 \approx 0$, then $V_l{}^2 \approx 2V_l + 1$. It can yield $V_{l+1} = V_l - (r_l P_l + x_l Q_l)$ from $2V_{l+1} - 1 = 2V_l - 1 - 2(r_l P_l + x_l Q_l)$ based on (3).

Therefore, the DistFlow model can be simplified as:

$$P_{l+1} = P_l - p_{n,l} \quad (4)$$

$$Q_{l+1} = Q_l - q_{n,l} \quad (5)$$

$$V_{l+1} = V_l - (r_l \times P_l + x_l \times Q_l) \quad (6)$$

where $p_{n,l}$ and $q_{n,l}$ represent the active and reactive power injection at the node n along branch l.

Based on linearised DistFlow, it is easy to determine branch flow change due to nodal power changes. An index matrix, inspired by the power transfer distribution factor, is determined by the sensitivity of an injected nodal power on the changing branch power flow in (7). This index ($M_{n,l}$) is used to measure the imapct of the ES located at node n on branch l's flow.

$$M_{n,l} = \frac{\partial P_l}{\partial p_{n,l}} \quad (7)$$

B. Cumulant Method

Cumulants and moments can effectively characterise a probability density function (PDF). For example, for the normal distribution, the first order cumulant is its mean and the second order cumulant is the variance. For a random variable x, such as P_n, the load demand at node n, the moment generating function $\Phi_{P_n}(s)$ is:

$$\Phi_{P_n}(s) = E[e^{sP_n}] = \int_{-\infty}^{\infty} e^{sP_n} f_{P_n}(P_n)\, dP_n \quad (8)$$

where $f_{P_n}(P_n)$ is the PDF of P_n.

Based on the moment generating function, the cumulant generating function $\Psi_{P_n}(s)$ is:

$$\Psi_{P_n}(s) = ln\, \Phi_{P_n}(s) \quad (9)$$

By taking the n-th derivative of the moment and cumulant

generating function, the *n-th* order raw moment m_n and cumulant λ_n can be determined at s=0.

Variable P_l, the active power flow on branch l, can be aggregated by the linear combination of independent load at different nodes (P_{n_1}, P_{n_2} ... P_{n_m}). Thus, the moment generating function $\Phi_Z(s)$ can be determined as:

$$P_l = M_{1,l}P_{n_1} + M_{2,l}P_{n_2} + \cdots M_{m,l}P_{n_m} \tag{10}$$

$$\begin{aligned}\Phi_{P_l}(s) &= E[e^{sP_l}] = E\left[e^{s(M_{1,l}P_{n_1}+M_{2,l}P_{n_2}+\cdots M_{m,l}P_{n_m})}\right] \\ &= E\left[e^{s(M_{1,l}P_{n_1})s(M_{2,l}P_{n_2})+\cdots s(M_{m,l}P_{n_m})}\right] \\ &= \Phi_{P_n1}(M_{1,l}s)\Phi_{P_n2}(M_{2,l}s)\ldots\Phi_{P_nm}(M_{m,l}s)\end{aligned} \tag{11}$$

where $M_{n,l}$ is the linerised power flow index between nodal load and branches, determined by (7).

Therefore, the cumulant for variable P_n is:

$$\begin{aligned}\Psi_{P_l}(s) &= ln(\Phi_{P_l}(s)) \\ &= \Psi_{P_{n_1}}(a_1 s) + \Psi_{P_{n_2}}(a_2 s) + \cdots \Psi_{P_{n_m}}(a_m s)\end{aligned} \tag{12}$$

The *n*th-order cumulant of P_l can be computed by taking the *n*th derivative of $\Psi_{P_l}(s)$ respective to s at $s = 0$.

$$\begin{aligned}\lambda_n &= \Psi_{P_l}^{(n)}(0) \\ M_1^n\Psi_{P_{n_1}}^{(n)}(0) &+ M_2^n\Psi_{P_{n_2}}^{(n)}(0) + \cdots M_m^n\Psi_{P_{nm}}^{(n)}(0)\end{aligned} \tag{13}$$

C. Gram-Charlier Expansion Method

With the moment of load PDF generated in the previous section, Gram-Charlier expansion method is implemented, which allows the PDF to be expressed as a series composed of a standard normal distribution and derivatives. By applying Edgeworth form, the Gram-Charlier form can be determined by moments and cumulants, considering the additive property of cumulants. With the cumulants of distribution in the standard form, the exponential representation of the PDF is

$$f(P_n) = e^{(-\frac{\lambda_3}{3!}D^3+\frac{\lambda_4}{4!}D^4-\frac{\lambda_5}{5!}D^5+\cdots)}\beta(P_n) \tag{14}$$

$$\beta(P_n) = \frac{1}{\sqrt{2\pi}\sigma}e^{-\frac{(P_n-\mu)^2}{2\sigma^2}} \tag{15}$$

where D^n is the n-th order derivative of the unit normal distribution, λ_n is the n-th order cumulant, $\beta(P_n)$ is the normal distribution function with mean (μ) and variance (δ). In the normal distribution, the 1st order cumulant is μ and the 2nd order cumulant is δ^2.

Therefore, the exponential series is:

$$\begin{aligned}f(P_n) = \Bigg[1 &+ \frac{(-\frac{\lambda_3}{3!}D^3+\frac{\lambda_4}{4!}D^4-\frac{\lambda_5}{5!}D^5+\cdots)}{1!} + \frac{(-\frac{\lambda_3}{3!}D^3+\frac{\lambda_4}{4!}D^4-\frac{\lambda_5}{5!}D^5+\cdots)^2}{2!} + \\ &\frac{(-\frac{\lambda_3}{3!}D^3+\frac{\lambda_4}{4!}D^4-\frac{\lambda_5}{5!}D^5+\cdots)^3}{3!} + \cdots\Bigg]\beta(P_n)\end{aligned} \tag{16}$$

By expanding each term and grouping by the power of D, the PDF can be expressed as:

$$\begin{aligned}f(P_n) = \beta(P_n) &- \frac{\lambda_3}{3!}D^3\beta(P_n) + \frac{\lambda_4}{4!}D^4\beta(P_n) - \frac{\lambda_5}{5!}D^5\beta(P_n) + \\ &\left(\frac{\lambda_6}{6!} + \frac{{\lambda_3}^2}{2!3!^2}\right)D^6\beta(P_n) - \left(\frac{\lambda_7}{7!} + \frac{2\lambda_3\lambda_4}{2!3!4!}\right)D^7\beta(P_n) + \cdots\end{aligned} \tag{17}$$

D. PV Output Modelling

The uncertainty in the probabilistic power flow is mainly from flexible load and renewable, where the renewable is considered as PV in this paper. The PV output uncertainty comes from the irradiance, which highly depends on the weather. The PV output is considered as $\pm 5\%$ of the predicted value. The hourly predicted power output of PV generation (P_{pv}) model [27] is introduced as:

$$P_{pv} = \gamma \times A_s \times G_0 \times \int_0^1 f(G/G_0; \varphi_G; \sigma_G) \tag{18}$$

where γ is the PV efficiency; A_s is the array surface area; G is the global horizontal irradiance; G_0denotes the corresponding extra-terrestrial irradiance; φ_G and σ_G can be estimated through fitting Beta distribution into the historical hourly solar irradiance data.

III. Operation Model for Energy Storage

This section designs the ES C/D method to reduce power flow variances of all branches to lower investment and congestion cost.

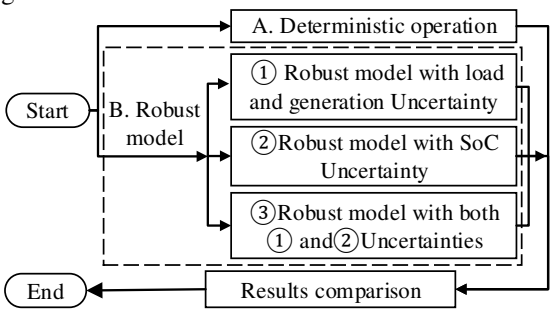

Fig.1. The flowchart of the ES operation model

The flowchart in Fig.1 shows the whole process of the ES operation by using different methods. There are two strategies: the deterministic model and the robust model. The deterministic model is solved by mixed integer quadratic programming (MIQP), which schedules the ES without considering uncertainties. In the robust model, there are three types of detailed robust models, listed in ①~③.

- Model ① applies robust optimisation, only considering uncertainty from load and renewable energy.
- Model ② only considers ES SoC uncertainty.
- Model ③ integrates load, renewable and ES SoC uncertainties.

The uncertainties from the flexible load and renewable energy are converted into power flow uncertainties by using the probabilistic power flow. Then, a comparison of these four models and ES status are analysed.

A. Deterministic Model

The objective function is to minimise system congestion using the least-square concept, achieved by reducing the variance of branch power flows, which is determined by the difference between the power flow at each time and its daily average. Because the reinforcement cost of each branch is different, a penalty factor is introduced to ensure ES operation to reduce the congestion according to the priority of branch costs. The problem is modelled as a mixed integer quadratic optimisation, which has three advantages: 1) to perform efficient peak shaving, which can obtain the lowest peak branch power flow after ES operation; 2) to give the priority to the branches that have high asset reinforcement costs to trigger ES discharging; and 3) to determine valley periods of the lowest load to charge the ES.

Obj:

$$Min: \quad \sum_{l=1}^{N} Asset_l \times [\sum_{t=1}^{T} \frac{1}{T}(pf_{e(l,t)} - Apf_l)^2] \tag{19}$$

s.t.:

$$pf_{e(l,t)} = pf_{l,t} + M_{n,l,t} \times (\frac{P_{c,t}}{\eta_{c,t}} - P_{d,t} \times \eta_{d,t}) \tag{20}$$

$$\mathrm{SoC_t} = \mathrm{SoC_{t-1}} + \frac{\mathrm{P_{c,t-1}} - \mathrm{P_{d,t-1}}}{\mathrm{C_{es}}} \tag{21}$$

$$0 \le \eta_{c,t} \le 1 \tag{22}$$

$$0 \le \eta_{d,t} \le 1 \tag{23}$$

$$SoC_t \le SoC_{max} \tag{24}$$

$$-SoC_t \le -SoC_{min} \tag{25}$$

$$P_{c,t} \le O_{rate} \tag{26}$$

$$P_{d,t} \le O_{rate} \tag{27}$$

$$P_{c,t} \le B \times C_{es} \qquad B \in (0,1) \tag{28}$$

$$P_{d,t} \le (1 - B) \times C_{es} \qquad B \in (0,1) \tag{29}$$

where, (20-21) are equality constraints of branch power flow, (21) describes the ES SoC based on the previous state, (22-27) are inequality constraints of efficiency, SoC, and storage C/D, and (28-29) are the constraints for the integer definition.

- $pf_{e(l,t)}$ is the power flow on branch l at time t after ES operation and Apf_l is the average power flow during period T on branch l.
- C_{es} is the storage capacity; SoC_t is the SoC of the storage; $P_{c,t}$ and $P_{d,t}$ are the charging and discharging amount of energy at time t.
- $M_{n,l,t}$ is branch flow sensitivity factor derived from DistFlow model.
- $pf_{l,t}$ is the original power flow without ES operation; η_c and η_d are the efficiency of ES during C/D.
- O_{rate} is the ES operation rete limitation.
- B is a *0,1* integer, which ensures there is no conflict for the C/D process of the ES system.

B. The Robust Model

The ES operation has uncertainties from four dimensions, which are 1) C/D length, 2) C/D time, 3) C/D amount, 4) SoC. The uncertainties of 1)~3) mainly come from the power flow uncertainties due to flexible load and renewable energy generation. These uncertainties are formed as the uncertainty sets in robust optimisation to minimise system peak and congestion. The severe case is the case where the uncertainty sets realise at the maximum magnitude of branch power flows, which leads to high system peak and large system congestions. In this paper, the severe case is the system condition with the highest branch flow resulted from the uncertainties of renewable generation, load and energy storage SOC, which lead to the largest system congestion. The upper boundary of the power flow is taken as the severe case in the study. The severe case under SoC uncertainty is that the SoC reaches 0.25 at the start of the day, which causes less capacity for charging during peak PV output periods.

The robust model is formulated as a min-max problem from a deterministic model. There are four typical uncertainty sets in robust optimisation, which are the interval uncertainty, ellipsoidal uncertainty, budgeted uncertainty, and norm uncertainty. The uncertainties in branch flows can be derived from load and renewable uncertainties based on the combined cumulant and Gram-Charlier expansion (8)~(18). With the same constraints in (20)~(29), the robust objectives and uncertainty sets can be derived. The robust optimisation is solved by using duality theory, which can convert the min-max robust problem into a MIQP problem.

• *Robust model with load and renewable uncertainty*

The uncertainty set only considering the uncertainty of branch power flow can be described in (31), which is formed as a budgeted uncertainty set. It also reduces the conservativity of robust optimisation. The objective function and the uncertainty set are

$$\underset{\mathrm{pf_{e(l,t)}}, SoC_t, Pc_t, Pd_t}{Min} : \underset{pf_{l,t}}{Max} : \sum_{\mathrm{l}=1}^{\mathrm{N}} Asset_l \times [\sum_{t=1}^{T} \frac{1}{T}(pf_{e(l,t)} - Apf_l)^2] \tag{30}$$

$$U_1 = \{\mathrm{pf_{l,t}} \mid \mathrm{pf_{l,t}} = \overline{\mathrm{pf_{l,t}}} + \xi_{l,t}, \widehat{\mathrm{pf_{l,t}}}, -1 \le \xi_{l,t} \le 1, \textstyle\sum_{t=1}^{24} \xi_{l,t} = \Gamma_l\} \tag{31}$$

where $\overline{pf_{l,t}}$ is the forecasted value of power flow derived from predicted load and renewable, $\widehat{pf_{l,t}}$ is the power flow deviation resulting from uncertainty on branch l at time t. $\xi_{l,t}$ and Γ_l show the conservation level of the ES operator.

• *Robust model with ES SoC Uncertainty*

With only SoC uncertainty, the objective function determines the minimum variance of daily branch power flow under the maximal impact of uncertainty in starting SoC. Because the starting SoC is decided by the end SoC on the previous day, it is impractical to define it as a constant value. Thus, the uncertainty set of the starting SoC is described as an interval uncertainty set. For example, if the starting SoC is high, the available capacity is lower, which means the ES has less capability to reduce the uncertainties by absorbing PV energy.

Thus, the objective function is formed as:

$$\min_{\mathrm{pf}_{e(l,t)}, SoC_{2:24}, Pc_t, Pd_t} : \max_{SoC_1} : \sum_{l=1}^{N} Asset_l \times [\sum_{t=1}^{T} \frac{1}{T} (pf_{e(l,t)} - Apf_l)^2] \quad (32)$$

$$U_2 = \{SoC_1 \mid SoC_1 \in [\overline{SoC_1} - \xi_1, \overline{SoC_1} + \xi_1]\} \quad (33)$$

where the $\overline{\mathrm{SoC}_1}$ is the forecast value of the start SoC, ξ_1 is the deviation at this time.

- *Robust model with ES SoC Uncertainty, load and renewable uncertainties*

The objective function is to minimise the variance of daily power flow from each branch under the maximal impact of uncertainties from starting SoC status, load and renewable output.

Thus, the objective function can be formed as:

$$\min_{\mathrm{pf}_{e(l,t)}, SoC_{2:24}, Pc_t, Pd_t} : \max_{SoC_1, pf_{l,t}} : \sum_{l=1}^{N} Asset_l \times [\sum_{t=1}^{T} \frac{1}{T} (pf_{e(l,t)} - Apf_l)^2] \quad (34)$$

$$U_3 = \{pf_{\mathrm{l,t}}, SoC_1 \mid U_1 + U_2\} \quad (35)$$

The uncertainty sets of power flow and initial SoC are described in (31, 33).

IV. Case Study

The proposed models are demonstrated on a practical GSP connected the UK distribution network in Fig.2 [29]. It is assumed that the ES is located at busbar 1007 with capacity 6MWh according to the peak output of PV at bus 1005. The generation on busbar 1005 (G1) is a PV farm, which supports demand during the daytime. Based on (18), the daily output of PV is depicted in Fig.3, with a peak of 25WM. G2 is at connected at busbar 1003 and the upstream system at the slack busbar 1008 is treated as G1008. The flexible load and renewable energy at each time point are assumed as uncertainty sets with $\pm 5\%$ boundary of the predicted value.

To simplify the analysis, the following assumptions are adopted: i) the efficiency of ES is 90%; ii) the minimum and maximum SoC levels are 0.2 and 0.8 respectively; iii) the capacity of the ES is 6MWh and its hourly max input/output power is 2 MW; iv) the uncertainty set boundary for the starting SoC is between 0.15 to 0.25.

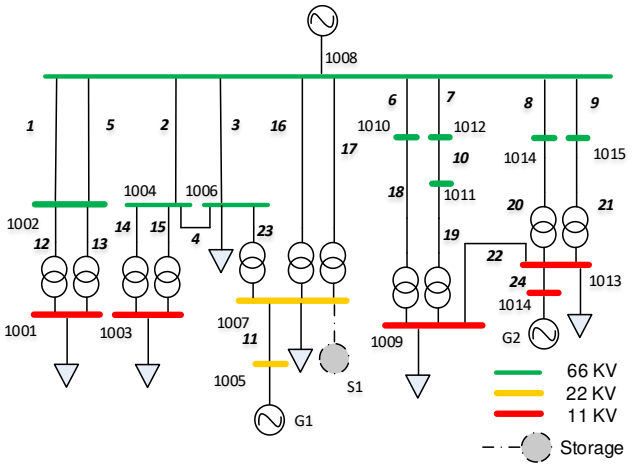

Fig.2. A Grid Supply Point (GSP) area test system.

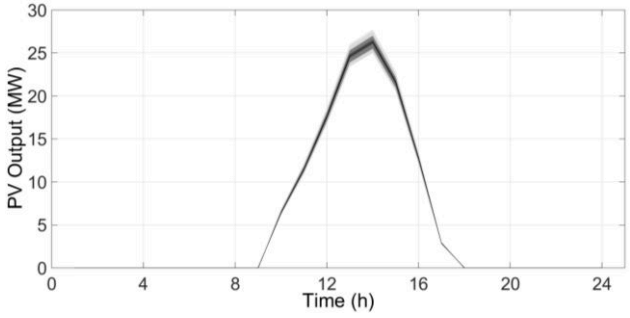

Fig.3. A daily PV output curve.

Table I shows the power flow capacity of each branch. The capacity of branches No.11 and No.24 is 50MW to accommodate renewable farms. Branch No.23 is the interconnector between two areas, which has the capacity of 6.5MW. The branch No.2 has the highest asset cost, which is £1.75 million. This branch as the priority to trigger the ES operation to mitigates its congestions. The branches at low voltage levels and the transforms have the same cost, which is £0.44 million.

TABLE I
The capacity of each branch (MW)

Branch	Asset cost (£m)	Capacity	Branch	Asset cost (£m)	Capacity
No.1	1.00	20	No.13	0.44	15
No.2	1.85	24	No.14	0.44	16
No.3	1.48	24	No.15	0.44	16
No.4	0.32	10	No.16	0.44	10
No.5	1.01	15	No.17	0.44	10
No.6	1.75	15	No.18	0.44	17
No.7	1.75	10	No.19	0.44	17
No.8	0.45	15	No.20	0.44	20
No.9	0.60	15	No.21	0.44	20
No.10	1.17	15	No.22	0.44	30
No.11	0.32	50	No.23	0.44	6.5
No.12	0.23	15	No.24	0.44	50

The power flow change resulting from different model analysis will be demonstrated from four scenarios, which are: 1) the deterministic model without considering any uncertainties; 2) the robust model only considering SoC

uncertainty; 3) the robust model only considering the uncertainty from flexible load and PV; 4) the robust model considering both load, PV and SoC uncertainties. The impact of these four scenarios on branch power flows and system congestions will be analysed and compared.

A. *Deterministic Model Operation*

Under the deterministic model, the original power flow which determined before ES operation is compared with the power flow after ES operation. Fig.4 shows the power flow change on branch No 2, with the highest asset cost, on which power flow has the priority to trigger ES operation. The peak of this branch is reduced from 22.5MW at 20:00 to 22.1MW at 19:00. Simultaneously, the congestion on this branch reduces from 0.93MWh to 0.11MWh, which removes 88.2% of the branch congestions. The congestion of the branch can be evaluated by the difference between the capacity and the power flow without capacity constraints.

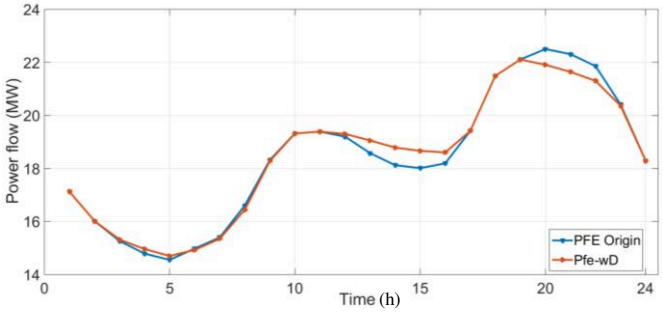

Fig.4. Power flow change on branch No.2

As shown in Fig.5, the original power flow is represented by the black curve and the power flow scheduled via the deterministic model is represented by the green curve. The branch flow peak is 7.0MW at 21:00, which is reduced to 6.7MW with the ES maximum discharging rate of 0.78MW/h. The congestion on this branch decreases from 0.47MWh to 0.25MWh and the system congestion, aggregating the congestions from all the branches, is reduced from 0.74MWh to 0.26MWh.

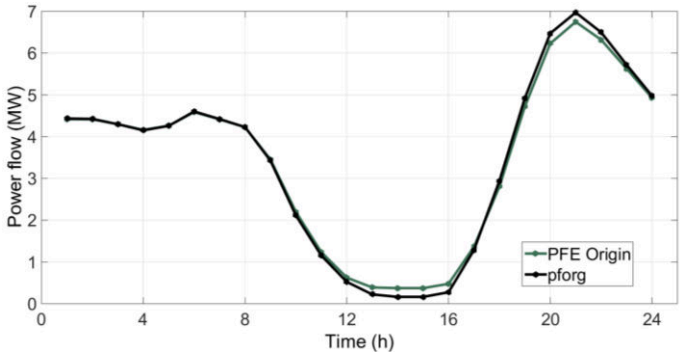

Fig.5. Power flow change on branch No.23 .

The C/D amount and the SoC of the ES in the deterministic model are shown in Fig 6. The ES is charging from 09:00 to 17:00 and discharging from 18:00 to 24:00. The maximum charging rate is 0.6MW/h at 14:00 and the maximum discharging rate is 0.8MW/h at 20:00. The SoC reaches 0.8 (the upper ES capacity limit) at 18:00, which is to prepare the following discharging process.

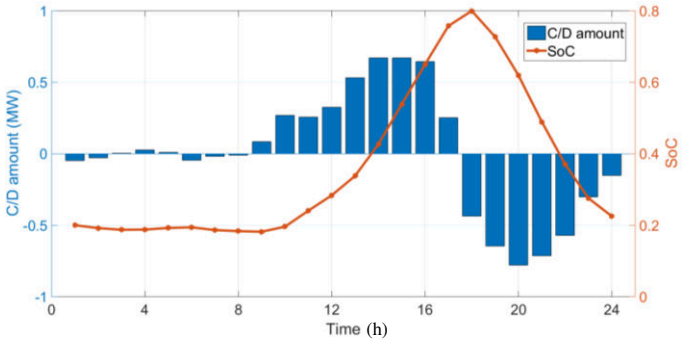

Fig.5. C/D and SoC in the deterministic model

B. *Robust Optimisation Considering Different Uncertainties*

The uncertainties from the load, PV and initial SoC are considered separately in this section. The power flow after ES operation in the severe case is analysed respectively corresponding to each uncertainty set in Fig.6.

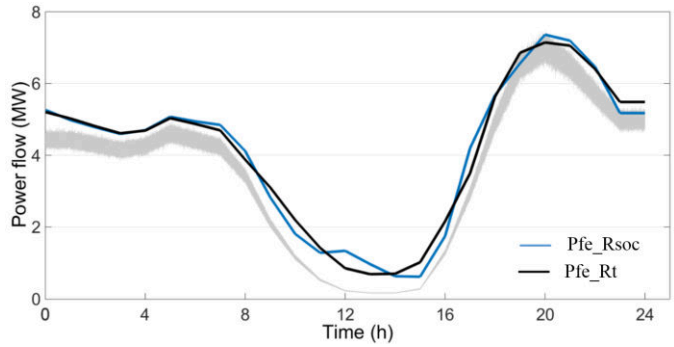

Fig.7. The impact of power flow on branch No.23 with SoC, load and PV uncertainties

As shown in Fig. 7, the grey area represents the range of the probabilistic power flow on branch No.23. Under the severe case, the starting SoC of ES is 0.25 and the power flow in the peak period reaches the upper boundary of the uncertainty set. The blue curve represents the power flow scheduled by robust optimisation under SoC uncertainty (*Pfe_RSoC*), which is higher than that under load and PV uncertainty (*Pfe_Rt*) at the peak time. From 11:00 to 16:00, the *Pfe_RSoC* is discharging which is caused by the SoC constraints. In the severe case, the power flow after ES operation will be reduced to 7.14MW under load and PV uncertainty and reduced to 7.36MW under SoC uncertainty. Respectively, the congestions on branch No.23 are 1.56MWh under load and PV uncertainty and 1.61MWh under SoC uncertainty. Therefore, the robust model considering the load and PV uncertainties performs better than that considering SoC uncertainty, in terms of reducing more power flow peak and system congestions in the severe case.

C. *Comparison of the Robust and Deterministic Model at the Severe Condition*

Fig.8 compares the power flow reduction by ES C/D

operation methods determined from the deterministic model and robust model, considering the uncertainties of load, PV and SoC. *Pfe_Rall* represents the power flow after ES operation considering all of SoC, load and PV uncertainty. *Pfe_wD* represents the power flow after ES operation by the deterministic model. The peak of the branch power flow can be reduced to 7.19MW and 7.44MW in *Pfe_Rall* and *Pfe_wD* respectively. The remained congestion after ES operation is 1.56MWh in the robust model which is lower than that in *Pfe_wD* (1.86MWh).

Therefore, based on observed power flow reduction from these two models, the deterministic model performs severer than the robust model considering uncertainties.

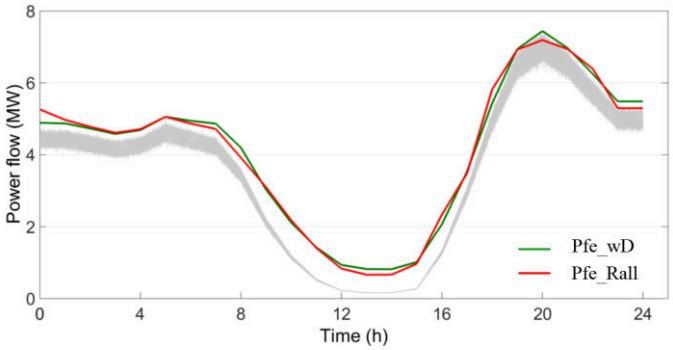

Fig.8. The power flow impact from the robust and deterministic model

D. *Comparison of C/D Method and SoC Change in Different Scenarios*

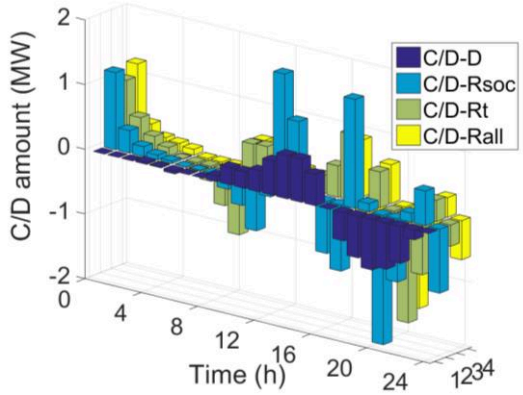

Fig.9. C/D amount at different scenarios

The C/D methods for the four scenarios are summarised and compared in Fig.9. Compared with the deterministic model determined C/D method (*C/D_D* in purple), the C/D methods determined by robust models are more fluctuated, especially the one determined by robust model only with SoC uncertainty (*C/D_Rsoc* in blue). The robust models determined C/D methods are more likely to charge at the beginning of the day. Only with SoC uncertainty, the maximum charging rate is 1.81MW/h at 13:00, which is proposed for the discharging and ensures the SoC not exceed its constraints. The maximum charging rate under load and PV uncertainty is 1.03MW/h at 17:00 and the maximum discharging rate is 1.67MW/h at 21:00. The maximum C/D rate of the robust model under all of the uncertainties (*C/D_Rall* in yellow) is 1.19MW/h at the start of the day and 1.52MW/h at 21:00 respectively. In the robust models, the maximum C/D rate is reduced from the model considering only ES SoC to the model considering all of the ES SoC, load and PV uncertainties. Although this means that the conservation of the robust models is increased, the robust models in high uncertainty cases reduce more system peak and congestions.

Fig.10 depicts the SoC change under these four scenarios. The SoC in the deterministic model (*SoC-D*) and the robust model considering SoC uncertainty (*SoC-Rsoc*) have a flat top. This is because they violent the SoC maximum constraints with their original C/D method. Thus, their SoC and C/D method is rescheduled. *SoC-D* reaches the maximum capacity of 0.8 from 17:00 to 18:00. *SoC-Rsoc* reaches the maximum capacity at 16:00 and 20:00. The robust model considering, load and PV uncertainty (*SoC-Rt*) and the model considering all the uncertainties (*SoC-Rall*) have similar profiles, which means the SoC uncertainty pose a slight impact on the ES operation. The *SoC-Rt* and *SoC-Rall* reach the maximum capacity at 18:00 and 20:00. Under uncertainties, the ES robust operation is conservative, which means the ES charges at the beginning of the day, from 00:00 to 06:00. This gives the ES have sufficient energy reserve to reduce the system congestions during the system peak periods.

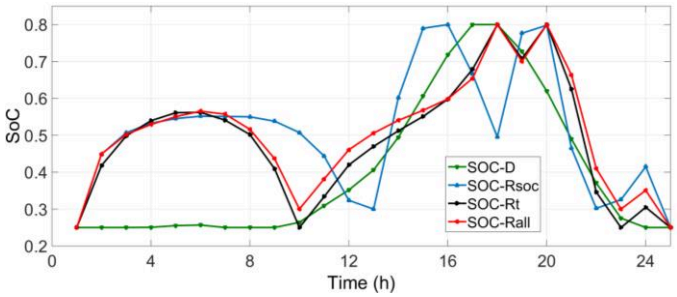

Fig.10. The SoC at different scenarios

TABLE II
THE SYSTEM CONGESTION IN DIFFERENT SCENARIOS

	Original	Deterministic	Robust SoC	Robust PV	Robust all
Congestion (MWh)	7.70	3.64	3.06	2.98	2.97

Table II shows the impacts of ES operation on the system congestion in the severe case. At this condition, the system congestion is 3.64MWh with the ES operation scheme determined by the deterministic model, which removes 52.73% congestions. This will decrease to 3.06MWh with the robust ES operation strategy considering SoC uncertainty. The robust optimisation with load and PV uncertainty set performs better, which reduces the congestion to 2.98MWh. When considering all of the SoC, load and PV uncertainties, the system congestion is reduced to 2.97MWh, which only 0.1% more than the model with load and PV uncertainty.

Therefore, the robust model considering all the uncertainties performs better than other models in the severe case. Considering the load and PV uncertainty, the robust model can reduce more congestions and branch peak than that considering SoC uncertainty individually. The congestion amount under the operation strategy determined by the deterministic model is

22% higher than the robust model with all the uncertainties.

V. Conclusions

This paper designs ES operation method using robust optimisation to mitigate system congestion by reducing the variance of daily branch power flow. Uncertainties from flexible demand, renewable energy generation, and ES SoC are modelled in the ES operation. This method could help network operators to plan and operate the ES to defer the system reinforcement and reduce system congestion. The following key findings are obtained:

- The power flow variance of the branch is reduced based on the least-square concept, which is able to guide ES operation to shift peak power flow and fill the demand valley efficiently;
- The robust optimisation is able to reduce system peak and system congestion in the severe case, and enable the network operator to reduce the peak power flow so as to decrease large-scale system investment;
- The ES SoC uncertainty poses less impact on branch power flows compared with the uncertainties from the flexible load and renewable energy generation.

This work is beneficial to the network operator to dispatch ES for the efficient support of system operation, such as congestion reduction and system peak management. Thus, the work can enable the existing system to accommodate increasing renewable generation and flexible demand with reduced investment costs.

References

[1] International Energy Agency, "IEA: Renewable electricity set to grow 40% globally by 2022," *https://www.carbonbrief.org/iea-renewable-electricity-set-to-grow-40-globally-by-2022,* 2017.

[2] E. Mearns, "UK Wind Constraint Payments," *http://euanmearns.com/uk-wind-constraint-payments/,* 2016.

[3] Y. Shi, B. Xu, D. Wang, and B. Zhang, "Using Battery Storage for Peak Shaving and Frequency Regulation: Joint Optimization for Superlinear Gains," *IEEE Transactions on Power Systems,* vol. 33, no. 3, pp. 2882-2894, 2018.

[4] J. Dong, F. Gao, X. Guan, Q. Zhai, and J. Wu, "Storage Sizing With Peak-Shaving Policy for Wind Farm Based on Cyclic Markov Chain Model," *IEEE Transactions on Sustainable Energy,* vol. 8, no. 3, pp. 978-989, 2017.

[5] N. Li and K. W. Hedman, "Economic Assessment of Energy Storage in Systems With High Levels of Renewable Resources," *IEEE Transactions on Sustainable Energy,* vol. 6, no. 3, pp. 1103-1111, 2015.

[6] A. Damiano, G. Gatto, I. Marongiu, M. Porru, and A. Serpi, "Real-Time Control Strategy of Energy Storage Systems for Renewable Energy Sources Exploitation," *IEEE Transactions on Sustainable Energy,* vol. 5, no. 2, pp. 567-576, 2014.

[7] Y. Zhang, N. Rahbari-Asr, J. Duan, and M. Y. Chow, "Day-Ahead Smart Grid Cooperative Distributed Energy Scheduling With Renewable and Storage Integration," *IEEE Transactions on Sustainable Energy,* vol. 7, no. 4, pp. 1739-1748, 2016.

[8] J. Yi, P. F. Lyons, P. J. Davison, P. Wang, and P. C. Taylor, "Robust Scheduling Scheme for Energy Storage to Facilitate High Penetration of Renewables," *IEEE Transactions on Sustainable Energy,* vol. 7, no. 2, pp. 797-807, 2016.

[9] M. Hajian, W. D. Rosehart, and H. Zareipour, "Probabilistic power flow by Monte Carlo simulation with Latin supercube sampling," *IEEE Transactions on Power Systems,* vol. 28, no. 2, pp. 1550-1559, 2013.

[10] Z. Xie, T. Ji, M. Li, and Q. Wu, "Quasi-Monte Carlo based probabilistic optimal power flow considering the correlation of wind speeds using copula function," *IEEE Transactions on Power Systems,* vol. 33, no. 2, pp. 2239-2247, 2018.

[11] H. Mori and W. Jiang, "A Markov-Chain Monte-Carlo technique for probabilistic load flow calculation," in *Circuits and Systems (MWSCAS), 2011 IEEE 54th International Midwest Symposium on*, 2011, pp. 1-4: IEEE.

[12] P. Zhang and S. T. Lee, "Probabilistic load flow computation using the method of combined cumulants and Gram-Charlier expansion," *IEEE transactions on power systems,* vol. 19, no. 1, pp. 676-682, 2004.

[13] A. Schellenberg, W. Rosehart, and J. Aguado, "Cumulant-based probabilistic optimal power flow (P-OPF) with Gaussian and gamma distributions," *IEEE Transactions on Power Systems,* vol. 20, no. 2, pp. 773-781, 2005.

[14] M. Fan, V. Vittal, G. T. Heydt, and R. Ayyanar, "Probabilistic power flow studies for transmission systems with photovoltaic generation using cumulants," *IEEE Transactions on Power Systems,* vol. 27, no. 4, pp. 2251-2261, 2012.

[15] A. J. Conejo, M. Carrión, and J. M. Morales, *Decision making under uncertainty in electricity markets*. Springer, 2010.

[16] D. Bertsimas and M. Sim, "The price of robustness," *Operations research,* vol. 52, no. 1, pp. 35-53, 2004.

[17] A. Ben-Tal, L. El Ghaoui, and A. Nemirovski, *Robust optimization*. Princeton University Press, 2009.

[18] W. Zheng, W. Wu, B. Zhang, and Y. Wang, "Robust reactive power optimisation and voltage control method for active distribution networks via dual time-scale coordination," *IET Generation, Transmission & Distribution,* vol. 11, no. 6, pp. 1461-1471, 2017.

[19] T. Ding, C. Li, Y. Yang, J. Jiang, Z. Bie, and F. Blaabjerg, "A two-stage robust optimization for centralized-optimal dispatch of photovoltaic inverters in active distribution networks," *IEEE Transactions on Sustainable Energy,* vol. 8, no. 2, pp. 744-754, 2017.

[20] B. Hu, L. Wu, and M. Marwali, "On the robust solution to SCUC with load and wind uncertainty correlations," *IEEE Transactions on Power Systems,* vol. 29, no. 6, pp. 2952-2964, 2014.

[21] H. Ye, J. Wang, and Z. Li, "MIP reformulation for max-min problems in two-stage robust SCUC," *IEEE Transactions on Power Systems,* vol. 32, no. 2, pp. 1237-1247, 2017.

[22] B. Hu and L. Wu, "Robust SCUC considering continuous/discrete uncertainties and quick-start units: A two-stage robust optimization with mixed-integer recourse," *IEEE Transactions on Power Systems,* vol. 31, no. 2, pp. 1407-1419, 2016.

[23] B. Zeng and L. Zhao, "Solving two-stage robust optimization problems using a column-and-constraint generation method," *Operations Research Letters,* vol. 41, no. 5, pp. 457-461, 2013.

[24] M. E. Baran and F. F. Wu, "Network reconfiguration in distribution systems for loss reduction and load balancing," *IEEE Transactions on Power delivery,* vol. 4, no. 2, pp. 1401-1407, 1989.

[25] L. Bai, J. Wang, C. Wang, C. Chen, and F. F. Li, "Distribution Locational Marginal Pricing (DLMP) for Congestion Management and Voltage Support," *IEEE Transactions on Power Systems,* 2017.

[26] H.-G. Yeh, D. F. Gayme, and S. H. Low, "Adaptive VAR control for distribution circuits with photovoltaic generators," *IEEE Transactions on Power Systems,* vol. 27, no. 3, pp. 1656-1663, 2012.

[27] X. Yan, C. Gu, H. Wyman-Pain, and F. Li, "Optimal Capacity Management for Multi-Service Energy Storage in Market Participation using Portfolio Theory," *IEEE Transactions on Industrial Electronics,* pp. 1-1, 2018.

[28] Y. Hongxia and J. Li, "A Survey of Robust Optimization," *ADVANCES IN MATHEMATICS (CHINA),* vol. 45, no. 3, 2016.

[29] X. Yan, C. Gu, F. Li, and Z. Wang, "LMP-Based Pricing for Energy Storage in Local Market to Facilitate PV Penetration," *IEEE Transactions on Power Systems,* vol. 33, no. 3, pp. 3373-3382, 2018.